# On the correlation between air-sea heat flux and abiotically induced oxygen gas exchange in a circulation model of the North Atlantic

H. Dietze and A. Oschlies[1]

Leibniz-Institut für Meereswissenschaften an der Universität Kiel, Kiel, Germany

Received 28 April 2004; revised 1 April 2005; accepted 25 May 2005; published 23 September 2005.

[1] The assumption that abiotic air-sea gas exchange is, via the temperature dependence of the gas' solubility, proportional to the surface heat flux is often used to distinguish between physically and biotically inferred oxygen fluxes across the sea surface. We quantitatively investigate its validity in the context of an eddy-permitting circulation model that contains an abiotic oxygen compartment. In the model, the "true" abiotic oxygen air-sea fluxes are systematically lower than those predicted by the air-sea heat flux relation. This discrepancy is caused by the nonlinear relationship between temperature and solubility that results in the saturation of a mixed water parcel being higher than the arithmetic mean saturation of the mixed components. This effect results in a simulated additional sea-to-air oxygen flux of about 0.5 mol $O_2$ $m^{-2}$ $a^{-1}$ north of 40°N, which is not accounted for by the heat-flux relation and which is of similar magnitude as, though at the lower end of, biotically induced oxygen fluxes. Simulated outgassing of the model's abiotic oxygen is also higher than that predicted by the heat-flux relation at the equator (by ≈0.25 mol $O_2$ $m^{-2}$ $a^{-1}$), where numerical artifacts endemic to state-of-the-art $z$ level ocean models are found to affect simulated air-sea gas exchange. In addition to discrepancies in the annual mean fluxes, model results also indicate that the subtropical seasonal cycle in abiotic air-sea oxygen exchange is smaller by approximately 20% than the estimate based on air-sea heat fluxes, a result consistent with admittedly sparse observations of argon saturation.

**Citation:** Dietze, H., and A. Oschlies (2005), On the correlation between air-sea heat flux and abiotically induced oxygen gas exchange in a circulation model of the North Atlantic, *J. Geophys. Res.*, *110*, C09016, doi:10.1029/2004JC002453.

## 1. Introduction

[2] To first-order approximation, the concentration of inert gases such as argon and neon, which do not have sources or sinks in the ocean interior, are close to solubility equilibrium with atmospheric concentrations throughout the oceans [e.g., *Hamme and Emerson*, 2002]. Hence the air-sea exchange of these gases is related to processes changing their solubility in the surface ocean, namely heat fluxes and (to a far lesser extent) freshwater fluxes.

[3] Accounting for the dominant role of temperature for variations of the solubility of inert gases under normal conditions, the total abiotically induced air-sea gas exchange, $F_{abiot}$, can be related to the local air-sea heat flux, $Q$, by

$$F_{abiot} \approx F_{therm} = +\frac{\partial C^{sat}}{\partial T}\frac{Q}{\rho\, c_p}, \qquad (1)$$

where $\partial C^{sat}/\partial T$ is the temperature derivative of the solubility of the respective gas, $c_p$ is the heat capacity and $\rho$ is the density of sea water.

[4] It is common practice to employ this relation to estimate air-sea gas exchange of inert (conservative) gases [e.g., *Bopp et al.*, 2002] and to separate physically and biotically affected air-sea exchange of oxygen [e.g., *Gruber et al.*, 2001; *Najjar and Keeling*, 2000; *Ganachaud and Wunsch*, 2002; *Keeling and Shertz*, 1992]. Because photosynthetic uptake of carbon dioxide is accompanied by oxygen release in a relatively fixed stoichiometric ratio, the biotically induced portion of air-sea fluxes of oxygen can be used to constrain estimates of the biological pump's impact on atmospheric carbon dioxide. Such applications implicitly assume that air-sea heat fluxes are the only physical forces driving air-sea gas exchange and that the kinetics of gas exchange are infinitely fast. These assumptions are violated by a number of abiotic processes, among them are (1) finite gas transfer velocity related to wind speed, waves and rain, (2) variations in atmospheric pressure, (3) subduction of air bubbles produced by waves, enhancing gas concentrations beyond saturation levels within the surface ocean, (4) interaction with sea ice and glacial ice [e.g., *Well and Roether*, 2003], and (5) variable bulk-skin temperature differences [e.g., *Donlon et al.*, 1999]. The present study does not address any of the above issues (even though they might be important), but instead focuses on the potential of (1) mixing in the ocean interior,

[1] Now at Southampton Oceanography Centre, Southampton, UK.


0148-0227/05/2004JC002453$09.00

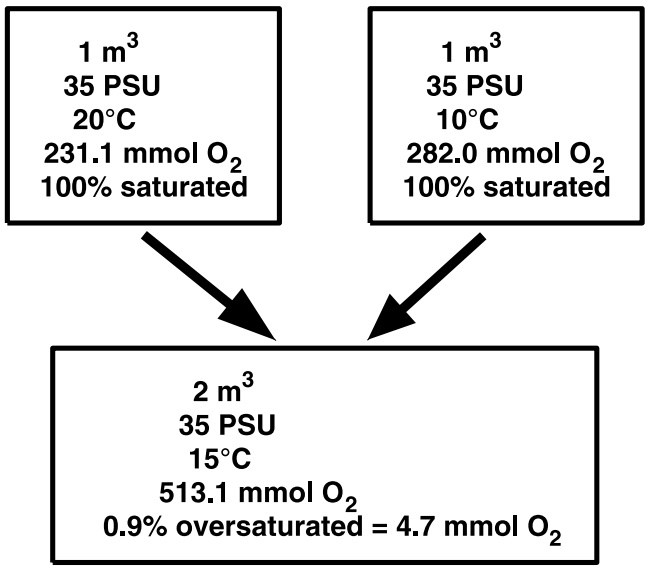


**Figure 1.** Mixing of two water parcels with different temperatures results in a mixed parcel oversaturated relative to the mean oxygen saturation of the original parcels.

and (2) solar radiation penetrating beneath the mixed layer to violate the above relation between abiotically induced air-sea gas exchange, $F_{abiot}$, and the local air-sea heat flux, $Q$.

[5] On the basis of measurements of noble gases in the Pacific and a one-dimensional diffusion-advection model, *Bieri et al.* [1966] concluded that mixing can cause significant oversaturation in the ocean interior. Although *Craig et al.* [1967] refuted both their measurements and their model results, diabatic mixing in the ocean interior will change the saturation level of dissolved gases whenever the relationship between solubility and temperature is nonlinear. As with regard to oxygen, mixing of two water parcels (irrespective of whether occurring along or across isopycnals) with different temperatures and salinities does always result in the mixed parcel being oversaturated relative to the mean saturation of the original parcels (see illustration in Figure 1). Whenever such a water parcel that was subject to intense mixing gets into contact with the atmosphere, more $O_2$ will outgas than predicted by the oxygen-to-heat flux relation (equation (1)). Although the resulting oversaturation is small (0.9% in the example illustrated in Figure 1) it might well affect air-sea oxygen fluxes by amounts similar to those induced by biological production. For example, a 200 m thick layer oversaturated by 0.9% before regaining contact with the atmosphere, for example, by being entrained into the winter mixed layer, will outgas an additional 1 mol $O_2$ $m^{-2}$ while typical biotically affected $O_2$ fluxes correspond to 2 mol $O_2$ $m^{-2}$ $a^{-1}$ [*Oschlies and Kähler*, 2004].

[6] Solar radiation penetrating below the mixed layer was already shown to cause subsurface supersaturation by *Spitzer and Jenkins* [1989]. On the basis of measurements of argon whose physical properties are close to those of oxygen, they reported an annual cycle of subsurface supersaturation in the subtropics. In spring/summer, water below the mixed layer is heated by solar radiation. As it warms, the solubility decreases and, once the water is shielded from the atmosphere, oversaturation evolves. When the mixed layer deepens because of destabilizing surface buoyancy fluxes during autumn/winter, the oversaturated water gets back into contact with the atmosphere. Thereby, penetrating solar radiation can seasonally decouple air-sea heat and abiotically affected oxygen fluxes.

[7] Here, both the effect of a seasonal decoupling of air-sea heat flux and abiotically induced gas exchange by penetrating solar radiation and the generation of a mean gas flux arising from mixing in the ocean interior will be examined quantitatively on a basin scale using an eddy-permitting ocean circulation model of the North Atlantic. After a brief description of the numerical model and the abiotic oxygen tracer used to quantify the above effects, regionally decoupled annual mean air-sea fluxes of heat and the abiotic oxygen tracer will be investigated in section 3. The seasonal decoupling is analyzed in section 4 and, after a discussion section, the paper ends with a summary of our findings.

## 2. Method

[8] An oxygen compartment, treated like an inert gas (e.g., argon), is embedded (online) into a circulation model identical to the one described by *Oschlies and Garçon* [1999]. The model covers the Atlantic Ocean between 15°S and 65°N with a grid spacing of 1/3° in meridional and 2/5° in zonal direction. The vertical grid has a total of 37 levels, 11 of these within the upper 150 m. Northern and southern boundaries are closed as is the Strait of Gibraltar. To account for water mass conversion outside the model domain, temperature and salinity are restored to values taken from the *Levitus* [1982] atlas in 5 grid point wide buffer zones, except for deep levels in the Denmark Strait where observational data are used to account for the signature of Denmark Strait Overflow Water [*Döscher et al.*, 1994]. An additional restoring zone off the Labrador shelf corrects for the missing sea-ice model and prevents the model from producing unrealistically cold water in winter.

[9] The atmospheric forcing consists of monthly mean wind stress and solar and nonsolar heat flux fields derived from the years 1989–1993 of the reanalysis project carried out at the European Centre for Medium-Range Weather Forecasts (ECMWF) [*Gibson et al.*, 1997]. Freshwater fluxes are parameterized by restoring surface salinity to observed monthly means taken from the *Levitus et al.* [1994] atlas. The formulation of the surface heat flux follows *Haney* [1971]. Solar heat flux penetrates into the ocean. Absorption is parameterized by the analytical formula of *Paulson and Simpson* [1977] for clear ocean water (type I [after *Jerlov*, 1976]) unless stated differently.

[10] The abiotic evolution of the oxygen concentration $O_2$ is determined by an advective-diffusive equation similar to that of temperature and salinity:

$$\frac{\partial O_2}{\partial t} = -\nabla \cdot (\mathbf{u} O_2) - A_h \nabla^4 O_2 + \frac{\partial}{\partial z}\left(K_\rho \frac{\partial O_2}{\partial z}\right) - \frac{\partial}{\partial z} F_{SA} O_2 \quad (2)$$

where the first term on the right-hand side accounts for advection, the second accounts for biharmonic horizontal diffusion, and the third term represents vertical mixing with turbulent diffusion coefficient $K_\rho$. The last term accounts for

the sea-air oxygen flux and is nonzero only for the uppermost grid box.

[11] Advection of temperature, salinity and oxygen is modeled using central differences both in space and in time. This scheme is commonly implemented in ocean models (e.g., CANDIE [*Sheng et al.*, 1998], MIT [*Marshall et al.*, 1997], MOM [*Pacanowski and Griffies*, 1999], OPA [*Madec et al.*, 1998], POP [*Smith et al.*, 1992]) because of its conceptional simplicity, no implicit diffusion and $o(\Delta x^2)$ accuracy. A major drawback of this scheme is, however, its dispersive nature [e.g., *Webb et al.*, 1998] that, for typical grid resolutions and diffusion coefficients, gives rise to spurious overshoots and undershoots when sharp tracer gradients are advected [e.g., *Oschlies*, 1999]. In order to restrict the dissipation needed for numerical stability reasons to small scales (ideally the grid scale), the present model follows a procedure commonly employed for high-resolution models and uses lateral biharmonic friction and mixing (with diffusivity and viscosity coefficients of $A_h$ = $2.5 \times 10^{11}$ m$^4$ s$^{-1}$). This reflects the notion that mixing along (approximately horizontal) isopycnal surfaces occurs mainly through the action of eddies and thus is supposed to be explicitly resolved by the model. Note that the biharmonic approach itself is capable of producing undershoots and overshoots as well; that is, it does not necessarily mix downgradient so that "unmixing" can occur.

[12] Turbulent vertical diffusivities $K_\rho$ in the water column are parameterized using the Turbulent Kinetic Energy (TKE) closure of *Gaspar et al.* [1990] in the modified version presented by *Blanke and Delecluse* [1993]. Values of $K_\rho$ are always positive, and the implicit treatment of vertical diffusion cannot generate spurious unmixing.

[13] The advection scheme and the subgrid parameterizations used were shown to adequately simulate the seasonal mixed layer cycle and diffusion in the main thermocline [*Oschlies et al.*, 2000; C. Eden and A. Oschlies, Effective diffusivities in models of the North Atlantic. part I: Subtropical thermocline, submitted to *Journal of Physical Oceanography*, 2003, hereinafter referred to as Eden and Oschlies, submitted manuscript, 2003]. All simulations were integrated for 20 years starting from a common spun-up state of the circulation model and oxygen concentrations corresponding to 100% saturation. The abiotic model's oxygen tracer is reset to 100% saturation every time step (≈30 minutes) in the restoring zones of the circulation model.

[14] Three different formulations for the sea-air exchange of oxygen ($F_{SA}O_2$) are used: (1) instantaneous restoring of surface concentration to saturation mimicking infinitely fast sea-air gas exchange; (2) Instantaneous surface restoring in combination with additional artificial subsurface oxygen sinks which exactly compensate for supersaturation due to local (subsurface) radiative heating at every depth level (The magnitude of the subsurface sinks at respective depth levels is calculated according to the vertical derivative of equation (1). The net sea-air oxygen flux $F_{SA}O_2$ in units mol $O_2$ m$^{-2}$ a$^{-1}$ is, in this case, diagnosed as the sum of oxygen flux put into the uppermost grid box and the vertical integral of the artificial sinks distributed over subsurface grid boxes. This approach does not change the heating profile (i.e., the circulation remains unchanged), but exactly compensates the effect of subsurface heating by penetrative solar radiation on oxygen saturation levels.); and (3) the formulation proposed by the OCMIP-2 protocol (R. G. Najjar and J. C. Orr, Design of OCMIP-2 simulations of chlorofluorocarbons, the solubility pump and common biogeochemistry, 1998; available from the World Wide Web at http://www.ipsl.jussieu.fr/OCMIP):

$$F_{SA}O_2 = KW\left(O_2^{surf} - O_2^{sat}\right) \tag{3}$$

where $O_2^{sat}$ is the oxygen concentration corresponding to a 100% saturation according to *Garcia and Gordon* [1992], $O_2^{surf}$ is the simulated oxygen concentration in the uppermost grid box, and $KW$ is the piston velocity, calculated according to *Wanninkhof* [1992]:

$$KW = a\left(u^2 + v\right)\left(ScO_2/660\right)^{-1/2} \tag{4}$$

with coefficient $a$ = 0.337 cm s$^2$ h$^{-1}$ m$^{-2}$ (which was changed from the original value of 0.31 proposed by *Wanninkhof* [1992] by the OCMIP group so that their global mean air-sea $CO_2$ exchange matches the *Broecker et al.* [1986] radiocarbon-calibrated estimate of 0.061 mol C m$^{-2}$ a$^{-1}$ μatm$^{-1}$) and the Schmidt number of oxygen in seawater $ScO_2$ as a function of temperature as proposed by *Keeling et al.* [1998]. The square of monthly mean wind speed $u^2$ and the variance $v$ of wind speed computed over one month were calculated from ECMWF climatology (using the same database which drives the circulation model). A crude ice model switches off air-sea gas exchange whenever sea surface temperatures drop below −1.8°C.

[15] In the context of our abiotic model, abiotically affected oxygen anomalies $\Delta O_2$ are then defined as

$$\Delta O_2 = O_2 - O_2^{sat}, \tag{5}$$

where $O_2$ is the simulated oxygen concentration of the respective water parcel.

[16] At every face of every model grid box (excluding the faces that make up the sea surface), the flux of oxygen anomalies $F\Delta O_2^{trans}$ (i.e., the combined effect of salt, heat and oxygen fluxes causing deviations from saturation) due to transport mechanisms *trans* defined below are calculated according to

$$F\Delta O_2^{trans} = FO_2^{trans} - \frac{\partial O_2^{sat}}{\partial T}\frac{Q^{trans}}{\rho c_p} - \frac{\partial O_2^{sat}}{\partial S}FS^{trans} \tag{6}$$

where $\partial O_2^{sat}/\partial T$ and $\partial O_2^{sat}/\partial S$ are temperature and salinity derivatives of the solubility of oxygen. $\rho c_p$ is the density times the heat capacity of seawater, and $Q^{trans}$, $FS^{trans}$, $F_2O^{trans}$ are heat, salt and oxygen fluxes across the same grid box face, respectively. For the respective transport mechanisms *trans*, we distinguish between oxygen anomaly fluxes due to horizontal ($F\Delta O_2^{ah}$) and vertical ($F\Delta O_2^{av}$) advection, as well as horizontal ($F\Delta O_2^{dh}$) and vertical ($F\Delta O_2^{dv}$) diffusion. The benefit of this oxygen anomaly flux concept is that the sum of the vertical integral of the flux divergences and the time derivative of the water column's

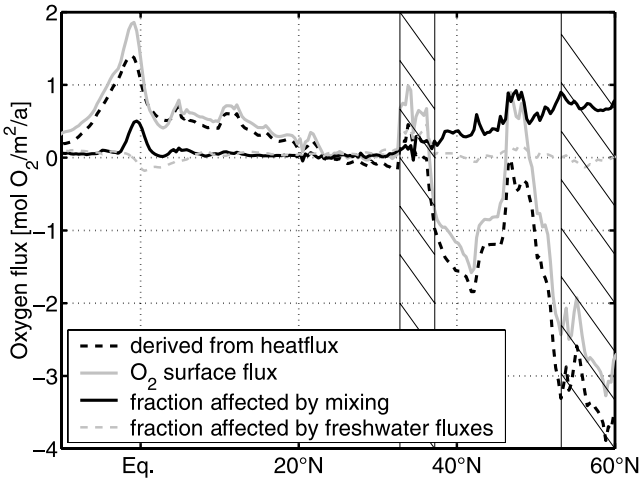


**Figure 2.** Zonal average of annual mean abiotically induced oxygen surface fluxes. Positive values indicate oceanic oxygen release. Solid gray line denotes the modeled air-sea flux. Dashed black line is air-sea oxygen flux derived from heat flux according to equation (1). Solid black line is the fraction of modeled air-sea flux attributed to mixing and gray dashed line is the fraction affected by air-sea freshwater fluxes. Shaded regions correspond to the latitudes of restoring zones (Strait of Gibraltar and Labrador Sea).

oxygen content yields the air-sea exchange of the abiotically affected oxygen anomaly. This enables us to decompose the modeled air-sea exchange of oxygen into the respective transport mechanisms driving the air-sea flux.

[17] Note that the separation between advective and diffusive fluxes is to some extent arbitrary: From a Lagrangian point of view it is evident that advection can neither be a source nor a sink for oxygen anomalies (i.e., deviations from saturation) while diffusion (i.e., mixing) is capable of producing oversaturation because of the nonlinear relationship between the solubility of oxygen and temperature/salinity. In ocean models that solve the Reynolds-averaged equations in an Eulerian framework, the distinction between advection and diffusion is problematic. Numerically, both advection and diffusion result in a partial mixing of adjacent boxes, depending on property gradients, flow rate, and diffusivity, respectively. This means that advection in the model is not only redistributing oversaturated water, but might as well be a source of oversaturation. As will be discussed later, the production of overshoots and undershoots by dispersive advection schemes may also generate oversaturation or even undersaturation.

## 3. Regionally Decoupled Air-Sea Heat and Oxygen Fluxes

[18] In the following, the impact of interior ocean mixing on air-sea oxygen fluxes is investigated in the coupled oxygen circulation model described in the previous section. The air-sea oxygen flux is modeled such that the potential effects of radiative subsurface heating and finite gas exchange are eliminated (formulation 2 of section 2). In this configuration, air-sea oxygen exchange is driven solely by changes in the solubility of oxygen affected by mixing, air-sea heat exchange, and freshwater fluxes.

[19] Figure 2 shows the zonal average of the modeled air-sea oxygen exchange for this scenario. Qualitatively it is correlated to the heat flux as proposed by equation (1): Warming in the tropics coincides with oceanic outgassing, and cooling in higher latitudes comes along with oceanic oxygen uptake. On quantitative terms, however, it is apparent that the abiotic oxygen air-sea flux estimated from the surface heat-flux relation (1) is systematically larger than the "true" air-sea flux simulated by the model. In the equatorial region the effect of mixing enhances oceanic outgassing by up to 0.25 mol $O_2$ $m^{-2}$ $a^{-1}$. At 48°N the effect is strongest, attenuating the zonally averaged oceanic oxygen uptake by up to 0.8 mol $O_2$ $m^{-2}$ $a^{-1}$, so that the sign of air-sea gas exchange is reversed relative to the estimate based on the surface heat flux.

[20] The spatial distribution of the modeled air-sea oxygen flux induced by mixing shows a distinct horizontal pattern (Figure 3). Most of the oversaturation is produced in the Gulf Stream and its extension where warm waters of the Gulf Stream mix with cold waters of the Labrador Current, and in the equatorial region. Integrated from 24°N to 48°N, the effect of mixing amounts to a deviation of the heat flux–derived abiotic oxygen flux from the "true" one by 162 kmol $O_2$ $s^{-1}$. This is larger than the difference between heat flux–derived and transport-derived $O_2$ fluxes attributed by *Ganachaud and Wunsch* [2002] to the biological pump.

[21] Partitioning the production of oversaturation into respective mechanisms reveals some insight into mixing processes at work (Figure 4). Note that it is impossible to

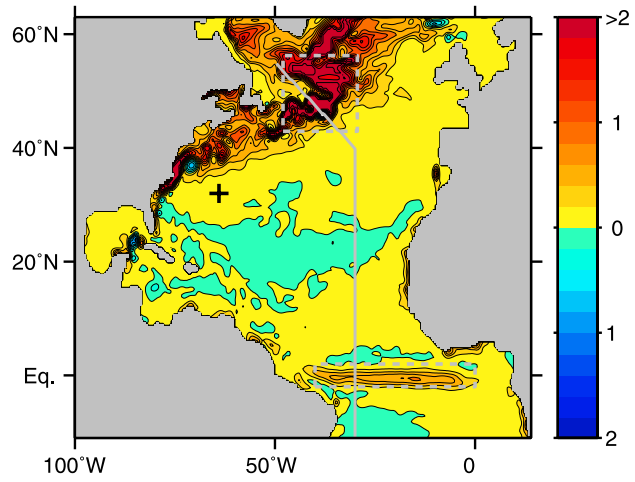


**Figure 3.** Fraction of modeled air-sea oxygen flux induced by mixing (annual mean). Units are mol $O_2$ $m^{-2}$ $a^{-1}$; positive values denote regions where oceanic outgassing is increased or oceanic oxygen uptake is subdued by mixing. Horizontal smoothing was applied (boxcar type with a filter width of ≈1.5°). Black cross indicates the position of station S. Dashed boxes bound the regions termed "equatorial" and "northern" box. Gray line indicates the course of the vertical section contoured in Figure 7.

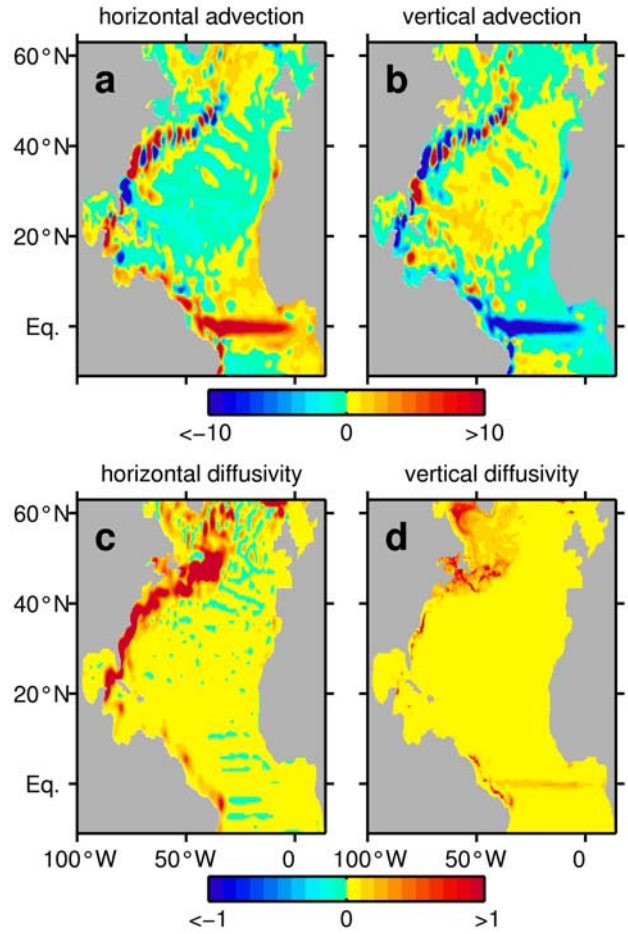


**Figure 4.** Vertical integrals of annual mean divergences of oxygen anomaly fluxes inferred by respective mechanisms, i.e., fraction of air-sea oxygen exchange induced by (a) horizontal advection, (b) vertical advection, (c) horizontal diffusivity, and (d) vertical diffusivity. Units are mol $O_2$ $m^{-2}$ $a^{-1}$; positive values denote processes increasing oxygen saturation, thus driving an oceanic oxygen loss. Horizontal smoothing was applied (boxcar type with a filter width of ≈1.5°).

produce undersaturation by mixing. Because of the nonlinear dependence of solubility on temperature (and to a much lesser extent salinity), a mixed water parcel always ends up being oversaturated relative to the arithmetic mean of the saturation of the original parcels. Hence the only process capable of producing undersaturation is "unmixing" which, in the model, results from dispersive numerical algorithms. Figure 4b shows the vertically integrated divergence of the oxygen flux anomalies affected by vertical advection. Positive values denote production of oversaturation, mirroring the mixing effect of advection explained in section 2. Negative values correspond to the production of undersaturation by "unmixing" and can be found in the equatorial region. This "unmixing" is a spurious effect of the advection scheme used and indicates the generation of overshoots and undershoots produced by numerical dispersion.

[22] Quantifying the net contribution of dispersion is not straightforward, and we are not aware of a method to locally isolate the numerical artifacts. Results of budget calculations shown in Table 1 give some idea about their magnitudes: in the "equatorial box" marked in Figure 3, the effect of horizontal and vertical advection on oxygen saturation are each two orders of magnitude larger (but of opposite sign) than the combined effect of horizontal and vertical mixing. While horizontal advection generates oversaturation, as would be expected from mixing, vertical advection generates undersaturation, which is definitely caused by numerically induced unmixing. In the "northern box", where Gulf Stream waters mix with waters of the Labrador Current, the spurious unmixing by horizontal advection is an order of magnitude smaller than the unmixing by vertical advection in the "equatorial box".

## 4. Decoupled Air-Sea Heat and Oxygen Fluxes on Seasonal Timescales

[23] The previous section considered the production of oxygen saturation anomalies due to interior water mass conversion and its effect on annual mean air-sea fluxes of oxygen. Because of seasonal variations in mixed layer depth and in water mass formation and destruction, it is likely that the air-sea flux generated by these saturation anomalies shows seasonal variations that may be temporally decoupled from the seasonal cycle in the surface heat flux. A seasonal decoupling is also expected to result from the interaction of penetrating solar radiation with the seasonally varying depth of the surface mixed layer. The simulated seasonal cycle of the zonally averaged air-sea abiotic oxygen exchange is displayed in Figure 5a in form of a Hovmöller diagram. We again assume infinitely fast gas exchange and restore surface oxygen concentrations to saturation values at every time step. Accordingly, the modeled seasonal cycle shown in Figure 5a results from the combined effects of varying air-sea heat fluxes, varying air-sea freshwater fluxes, subsurface heating due to solar radiation, and interior ocean mixing. The effect of freshwater fluxes turns out to be negligible. Even the very large freshwater fluxes imposed by restoring to climatological surface salinities in the Amazonas inflow region add up to less than 0.2 mol $O_2$ $m^{-2}$ $a^{-1}$ in the annual mean zonal average (Figure 2), with seasonal variations being much smaller than the annual mean.

[24] When the abiotic air-sea oxygen fluxes are estimated from the instantaneous surface heat fluxes via relation (1), it turns out that the amplitude of the seasonal cycle in the physically driven portion of the ocean-atmosphere gas exchange is overestimated by typically 20–30%. The zon-

**Table 1.** Budget of Annual Mean Convergence of the Oxygen Anomaly Fluxes Within "Northern" and "Equatorial" Boxes Marked in Figure 3[a]

| Box | *ah* | *av* | *dh* | *dv* | Storage | ∑ |
|---|---|---|---|---|---|---|
| equat. | 490 | −475 | 2 | 7 | >−1 | 23 |
| northern | −16 | 30 | 60 | 10 | >−1 | 84 |

[a]Units are kmol $O_2$ $s^{-1}$. Positive numbers denote supersaturating effects of horizontal/vertical advection (*ah*, *av*) and horizontal/vertical diffusion (*dh*, *dv*), decreasing stock of supersaturation (*Storage*), and oceanic outgassing due to the combined effect (∑).

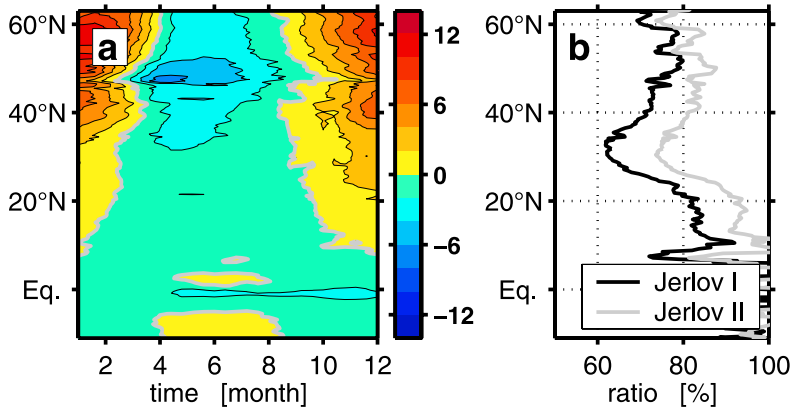


**Figure 5.** (a) Zonal mean of modeled abiotically induced air-sea oxygen flux. Units are mol $O_2$ $m^{-2}$ $a^{-1}$; negative numbers denote oceanic oxygen uptake. Absorption of solar radiation is parameterized using the optical water type I of *Jerlov* [1976]. (b) Zonally averaged seasonal amplitudes (first harmonic) of modeled air-sea oxygen fluxes relative to amplitudes derived from heat fluxes following equation (1). Types I and II refer to optical water types used in the respective model integrations.

ally averaged amplitudes are shown in Figure 5b for two different choices of Jerlov's optical water types [*Jerlov*, 1976] that describe attenuation of solar radiation in the water column. The overestimate is larger for type I waters which allow solar radiation to penetrate deeper into the ocean than type II waters. This can be explained by more radiative energy being stored seasonally in the depth range between the maximum depth of the winter mixed layer and the shallower summer mixed layers. The associated subsurface heating increases local saturation levels during summer, which result in additional air-sea oxygen fluxes when the water comes into contact with the atmosphere in the subsequent winter. Effects are largest between about 25°N and 40°N, where the zonal mean of *Jerlov*'s [1976] optical water types was estimated to lie somewhere in between type I and type II [*Simonot and Le Treut*, 1986]. Here, the heat flux–based gas exchange estimate on average overestimates the amplitude of the seasonal cycle by as much as 26% and 38% for optical water types II and I, respectively.

[25] In order to differentiate between the effects of mixing and subsurface solar heating on the seasonal cycle of air-sea gas exchange, additional model runs were performed with instantaneous surface restoring of oxygen to saturation values in combination with an artificial subsurface oxygen sink term that compensates for supersaturation due to subsurface solar heating (section 2). The difference between the air-sea oxygen exchange modeled in this way and the air-sea flux estimated from the model's surface heat flux (equation (1)) yields the effect of mixing only. The amplitudes of the respective seasonal cycles of the simulated air-sea oxygen flux are shown in Figure 6. It turns out that mixing and subsurface solar heating attenuate the seasonal cycle of air-sea oxygen exchange by roughly equal amounts (see also Table 2).

[26] The main mechanism behind the attenuating effect of "mixing" is related to mixed layer dynamics. In most regions of the model, the generation of oversaturation by mixing below the mixed layer is relatively constant in time and thus would impose a constant bias on air-sea oxygen exchange rather than a seasonal cycle opposing the fraction of air-sea exchange driven by the surface heat flux. Seasonal mixed layer dynamics, however, determine when the mixed and hence oversaturated water gets into immediate contact with the atmosphere. In the subtropics, mixed layers deepen during fall/winter when oceanic heat loss destabilizes the water column. During this cooling period, relation 1 proposes an oxygen flux into the ocean which is attenuated by

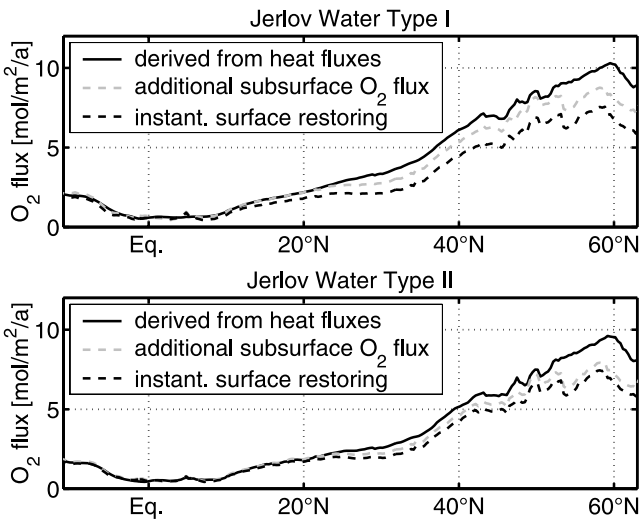


**Figure 6.** Zonally averaged seasonal amplitudes (first harmonic) of oxygen fluxes proposed by a suite of model integrations. Solid black lines refer to the propositions based on air-sea heat fluxes (equation (1)). Note that the air-sea heat flux is slightly dependent on the optical water type used to parameterize the absorption of solar radiation. Dashed black lines are for model integrations using an instantaneous restoring of surface oxygen concentrations to saturation values. Dashed gray lines refer to integrations with instantaneous surface restoring in combination with an artificial subsurface oxygen flux, which compensates for oversaturation due to solar subsurface heating.

**Table 2.** Attenuation of Seasonal Cycle in Air-Sea Oxygen Exchange Due to Respective Mechanism Relative to the Proposition Based on Heat Flux (Equation (1))[a]

| Optical Water Type of *Jerlov* [1976] | I | II |
|---|---|---|
| Mixing | 15.5% | 12.7% |
| Subsurface heating due to solar radiation | 18.6% | 9.9% |
| $\sum$ | 34.1% | 22.6% |

[a]The numbers refer to a subtropical average (25°N–40°N).

the entrained oversaturated water regaining contact with the atmosphere. Hence the effect of "mixing" on the seasonal cycle of air-sea oxygen exchange is related to mixed layer deepening in fall/winter.

[27] When switching from optical water type I to II, i.e., from deeper to shallower solar penetration, maximum mixed layer depths in winter tend to become shallower, while summer mixed layer depths stay relatively constant in the subtropics. Consequently, the attenuating effect of "mixing" on the seasonal cycle of air-sea oxygen exchange is slightly weaker for optical water type II than it is for optical water type I (Table 2).

## 5. Discussion

### 5.1. Regionally Decoupled Air-Sea Heat and Oxygen Fluxes

[28] Figure 4 epitomizes that mixing, as it occurs in an OGCM based on central differences, is a complex process that involves spurious numerical artifacts. In addition to the numerical advection scheme, horizontal biharmonic diffusion (as commonly employed in high-resolution models) is another source of numerical dispersion ("unmixing"). Moreover, dispersion effects may produce static instabilities, which in turn affect vertical diffusion schemes.

[29] It remains to be shown that the total mixing rates resulting from the various tracer transport schemes in OGCMs are realistic (which is not straightforward and beyond the scope of this work, but see Eden and Oschlies (submitted manuscript, 2003)). While measurements of transient tracers such as helium, tritium, CFCs and purposefully deployed $SF_6$ have already been proven to be a valuable base for model evaluation, we propose that the comparison with argon measurements would be of additional benefit for the OGCM community: Argon is an inert gas whose distribution is solely controlled by physical processes. Wherever argon supersaturation shows up in the deep ocean, mixing must have occurred to the extent that other diabatic processes or bubble entrainment at the surface can be ruled out. As the physical properties of argon are close to those of oxygen, its distribution should mirror the abiotic oxygen distribution.

[30] Figure 7 shows a vertical section of modeled (annual mean) oxygen saturation through the North Atlantic (along the transect marked in Figure 3). If modeled mixing rates are realistic, the effect of mixing on argon supersaturation is larger than the measurement accuracy of argon supersaturation (which is ±0.1–0.3% deviation from saturation according to *Emerson et al.* [1999]).

[31] What we report here is that a state-of-the-art eddy-permitting model predicts significant production rates of oversaturation due to diabatic mixing in various regions. This is most pronounced in the Gulf Stream and its extension, where the warm return flow of the thermohaline circulation entering the subpolar gyre mixes with cold surrounding water before or while air-sea heat fluxes increase its density so that the water can sink and become part of the deep water masses again. In addition, high rates of diapycnal mixing in the Gulf Stream have been suggested to supply nutrients into the euphotic zone and to be a major contributor for fueling new production in the subtropical gyre of the North Atlantic [*Jenkins and Doney*, 2003].

[32] As with regard to the oversaturation simulated by the model, a rough calculation supports the hypothesis that mixing significantly contributes to local air-sea exchange of oxygen: Following the calculation in Figure 1 and assuming that the Gulf Stream, which increases in transport from 30 Sv in the Florida Strait to 70–100 Sv at Cape Hatteras, after separation from the U.S. coast effectively mixes 32 Sv of 20°C warm water with 32 Sv of 10°C cold water yields a production of oversaturation corresponding to 150 kmol $O_2$ $s^{-1}$. To put this number in perspective it is helpful to compare it with the inversion of WOCE data. For the North Atlantic between 24°N and 48°N, *Ganachaud and Wunsch* [2002] propose a total oxygen gain due to the combined effect of biological and solubility pump of 600 ± 200 kmol $O_2$ $s^{-1}$, while an estimate based on heat flux alone (equation (1)) yields 750 ± 150 kmol $O_2$ $s^{-1}$ [*Ganachaud and Wunsch*, 2002]. Ignoring errors and assuming that the heat flux estimate accounts for all physical processes suggests a net biotic oxygen production of 150 kmol $O_2$ $s^{-1}$. Thus the effect of mixing on air-sea oxygen fluxes is not negligible and might, in this area, reverse the sign of biotic oxygen production estimates.

[33] The situation is somewhat different for mixing rates modeled in the equatorial region. Here, numerical artifacts of ocean models can lead to numerically generated unrealistic nitrate maxima in the eastern equatorial Atlantic [*Oschlies*, 2000]. Corresponding numerical effects may have an influence on simulated air-sea gas exchange of oxygen.

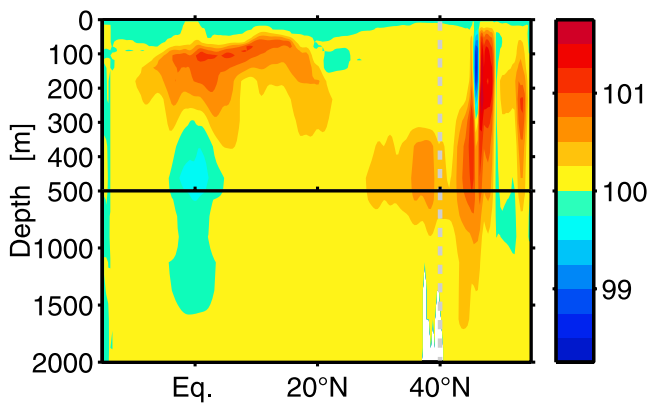


**Figure 7.** Section of abiotically induced annual mean oxygen saturation along the transect indicated in Figure 3. The vertical dashed line indicates change of course. Units are percent saturation.

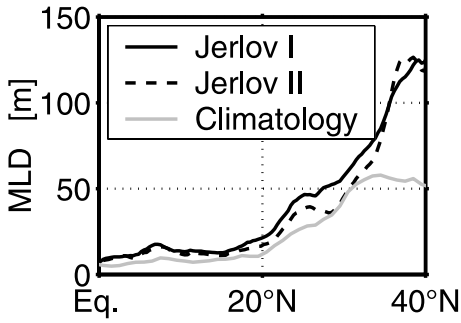


**Figure 8.** Zonally averaged seasonal amplitudes (first harmonic) of mixed layer depths, here defined as the depth where density $\sigma_0$ is 0.125 higher than at the surface. Black lines refer to model integrations. The black solid line was simulated using optical water type I to parameterize absorption of solar radiation, while the black dashed line was simulated using water type II. The gray line is derived from monthly climatologies of salinity and temperature [*Levitus et al.*, 1994; *Levitus and Boyer*, 1994].

[34] It is noteworthy that atmospheric models driven by biogeochemical ocean models predict an equatorial peak in atmospheric potential oxygen (APO $\approx O_2 + CO_2$ [*Stephens et al.*, 1998]). The definition of APO ensures that its atmospheric distribution is governed by the air-sea fluxes of $CO_2$ and $O_2$ because terrestrial $O_2$ and $CO_2$ fluxes tend to oppose each other. APO is more sensitive to the solubility pump, as air-sea $CO_2$ and $O_2$ fluxes affect it in the same direction, while the biological pumps of the respective gases oppose each other. Hence the modeled equatorial peaks will be correlated to the solubility pump. While all models we are aware of fail to reproduce the observed mean meridional APO gradient, a common and dominant signal is the large equatorial APO peak that, to our knowledge, has not yet been confirmed or rejected by observations. It may well be possible that deficiencies of the numerical models significantly affect the simulated APO patterns, particularly in the tropics.

### 5.2. Discussion of Modeled Seasonal Cycle of Air-Sea Oxygen Fluxes

[35] The attenuating effect of mixing on the seasonal cycle of air-sea oxygen exchange reported in the previous section is correct to the extent that mixing and the seasonal cycle of the mixed layer are realistically simulated by the model. It turns out that the seasonal cycle in subtropical mixed layer depths seems to be overestimated by the model when compared to the climatologies of *Levitus et al.* [1994] and *Levitus and Boyer* [1994] (Figure 8), although the climatological seasonal cycle of mixed layer depths might be biased low because of averaging artifacts.

[36] With respect to the attenuating effect of subsurface solar heating, model assessment is possible at a site in the subtropics (station S 32°N, 64°W, marked in Figure 3) where the seasonal cycle of argon oversaturation was measured in the upper part of the water column by *Spitzer and Jenkins* [1989]. Since argon is an inert gas whose physical properties are close to those of oxygen, observed argon oversaturation can be transferred into oxygen units. Figure 9 shows an intercomparison between the observations of *Spitzer and Jenkins* [1989] and results from a suite of model integrations:

[37] Simulated mixed layer depths agree well with observations during summer, irrespective of the optical water type used to parameterize absorption of solar radiation. Obviously, winter mixed layers are deeper in the simulations than in the observations, but this should not affect oxygen anomalies in summer. The quality of simulated mixed layers is mirrored in the sea surface temperature, that also shows good agreement with observations during summer and too low values in winter.

[38] Modeled oxygen anomalies at station S are predominantly affected by subsurface solar heating since the effect of mixing is small (Figure 3). During summer, best agree-

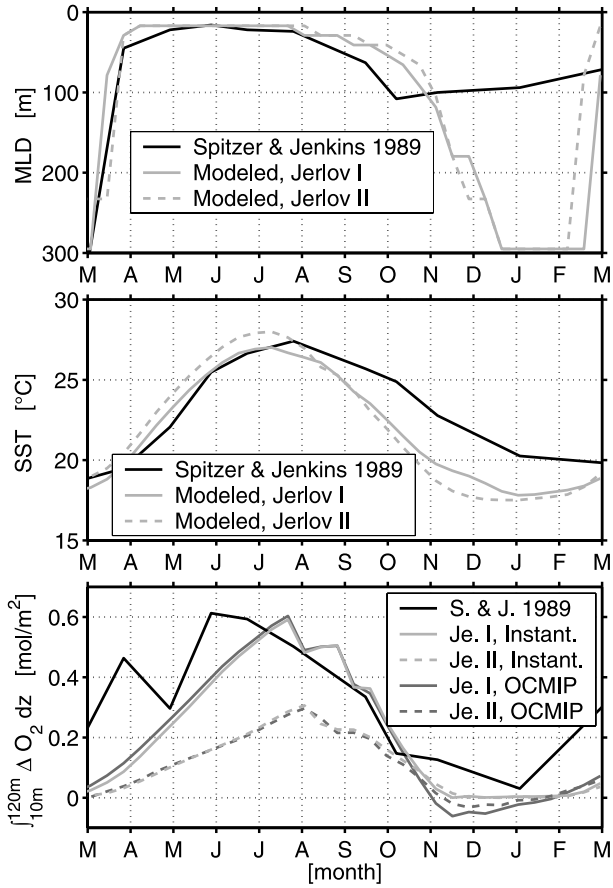


**Figure 9.** Intercomparison between observations of *Spitzer and Jenkins* [1989] and a suite of model integrations at station S (32°N, 64°W): (top) mixed layer depths, here defined as the depth where density $\sigma_0$ is 0.125 higher than at the surface, (middle) sea surface temperatures, and (bottom) abiotically induced oxygen anomalies integrated vertically between 10 m and 120 m. (Observed abiotically affected oxygen anomalies (black solid line in Figure 9 (bottom)) were derived from argon data.) Jerlov I and II refer to model integrations using respective optical water types to parameterize absorption of solar radiation. Instant. denotes integrations with instantaneous restoring of surface oxygen concentrations to saturation values. OCMIP denotes integrations where air-sea oxygen exchange was parameterized following the OCMIP-2 guideline (section 2).

ment with the observations is found for simulations that use optical water type I. Note, however, that this coincidence might well be for the wrong dynamical reason as the model has no representation of the effect of bubble entrainment, which *Spitzer and Jenkins* [1989] suggest to account for 40% of the oversaturation observed in summer. Keeping the neglect of bubble entrainment in mind, the somewhat lower oversaturation simulated by using the optical water type II may even be more consistent with observations.

[39] We conservatively conclude that the seasonal cycle of air-sea gas exchange is attenuated by about 10% (Table 2) because of subsurface solar heating in the subtropical North Atlantic, with mixing contributing an additional attenuation of approximately 10%. Note that this result is relatively insensitive to the actual formulation of the air-sea boundary condition for oxygen.

## 6. Summary

[40] Abiotically induced air-sea oxygen fluxes were studied in an eddy-permitting circulation model of the North Atlantic. The focus was on the quantitative validation of a relationship between air-sea heat fluxes and abiotically affected oxygen fluxes, a method often used to distinguish between the effects of the solubility pump and the biological pump on air-sea gas exchange of oxygen and carbon dioxide.

[41] A conservative interpretation of our model results, consistent with admittedly sparse observations of argon oversaturation, indicates that this method yields annual cycles of air-sea oxygen flux biased high by approximately 10% because of subsurface solar heating of water shielded from the atmosphere in spring/summer and subsequent mixed layer deepening in fall/winter which brings the (by then supersaturated) water back into contact with the atmosphere. While a neglect of subsurface heating by solar radiation leads to considerable overestimation of the seasonal $O_2$ flux cycle, errors should average out on the annual mean.

[42] Another caveat that does not average out on annual and longer timescales is that when estimating abiotically induced oxygen fluxes from surface heat fluxes, this method does not account for mixing processes that produce oversaturation because of the nonlinear dependence of oxygen saturation on temperature. While the production of oversaturation due to mixing in the ocean interior is relatively constant in time, mixed layer dynamics determine when the mixed and hence oversaturated water gets into immediate contact with the atmosphere. As a result, the impact of mixing on air-sea fluxes of oxygen also shows a pronounced seasonal cycle, particularly in the subtropics. The model results indicate that the neglect of the interplay between interior water mass transformation and mixed layer dynamics overestimates the amplitude of the seasonal cycle at least by another 10% in the subtropical North Atlantic.

[43] With respect to annual mean fluxes, the model predicts that oceanic oxygen outgassing at the equator is enhanced by $\approx$0.25 mol $O_2$ $m^{-2}$ $a^{-1}$ and oceanic oxygen uptake north of 40°N decreases by $\approx$0.5 mol $O_2$ $m^{-2}$ $a^{-1}$ as a result of mixing. Biotically affected air-sea exchange in the North Atlantic corresponds to about 2 mol $O_2$ $m^{-2}$ $a^{-1}$ [*Oschlies and Kähler*, 2004] (based on model results). Thus modeled oxygen fluxes induced by mixing amount to $\approx$25% of the biotic estimate north of 40°N.

[44] We presented evidence that simulated abiotic air-sea oxygen fluxes are considerably influenced by numerical artifacts, particularly along the equator. Unfortunately, we could not validate the net mixing present in the model as particularly the diabatic mixing rates in regions with strong currents are not yet well constrained. However, model results presented in this study reveal that measurements of inert gases with nonlinear solubility-to-temperature relation may help to constrain diabatic mixing in the ocean interior since the subsurface mixing history of a water parcel leaves its imprint on the saturation. Thus we expect that more comprehensive data sets of, for example, argon or neon measurements will help to locate water mass conversion in the ocean interior, which in steady state, has to balance water mass formation at the sea surface.

[45] **Acknowledgments.** We acknowledge funding by the Deutsche Forschungsgemeinschaft and discussions with Carsten Eden. Very constructive and helpful comments of two anonymous reviewers helped to improve the paper.

## References

Bieri, R. H., M. Koide, and E. D. Goldberg (1966), The noble gas contents of Pacific seawaters, *J. Geophys. Res.*, *71*, 5243–5265.

Blanke, B., and P. Delecluse (1993), Variability of the tropical Atlantic Ocean simulated by a general circulation model with two different mixed-layer physics, *J. Phys. Oceanogr.*, *23*, 1363–1388.

Bopp, L., C. L. Quéré, M. Heimann, A. C. Manning, and P. Monfray (2002), Climate-induced oceanic oxygen fluxes: Implications for the contemporary carbon budget, *Global Biogeochem. Cycles*, *16*(2), 1022, doi:10.1029/2001GB001445.

Broecker, W. S., J. R. Ledwell, T. Takahashi, R. Weiss, L. Merlivat, L. Memery, T.-H. Peng, B. Jahne, and K. O. Munnich (1986), Isotopic versus micrometeorologic ocean $CO_2$ fluxes: A serious conflict, *J. Geophys. Res.*, *91*, 10,517–10,528.

Craig, H., R. F. Weiss, and W. B. Clarke (1967), Dissolved gases in the equatorial and South Pacific Ocean, *J. Geophys. Res.*, *72*, 6165–6181.

Donlon, C. J., T. J. Nightingale, T. Sheasby, J. Turner, I. S. Robinson, and W. J. Emery (1999), Implications of the oceanic thermal skin temperature deviation at high wind speed, *Geophys. Res. Lett.*, *26*, 2505–2508.

Döscher, R., C. W. Böhning, and P. Herrmann (1994), Response of circulation and heat transport in the North Atlantic to changes in thermohaline forcing in northern latitudes: A model study, *J. Phys. Oceanogr.*, *24*, 2306–2320.

Emerson, S., C. Stump, D. Wilbur, and P. Quay (1999), Accurate measurement of $O_2$, $N_2$ and Ar gases in water and the solubility of $N_2$, *Mar. Chem.*, *64*, 337–347.

Ganachaud, A., and C. Wunsch (2002), Oceanic nutrient and oxygen transports and bounds on export production during the World Ocean Circulation Experiment, *Global Biogeochem. Cycles*, *16*(4), 1057, doi:10.1029/2000GB001333.

Garcia, H. E., and L. I. Gordon (1992), Oxygen solubility in seawater: Better fitting equations, *Limnol. Oceanogr.*, *37*, 1307–1312.

Gaspar, P. Y., Y. Gregoris, and J. M. Lefevre (1990), A simple eddy kinetic energy model for simulations of the oceanic vertical mixing: Tests at station Papa and Long-Term Upper Ocean Study site, *J. Geophys. Res.*, *95*, 16,179–16,193.

Gibson, J. K., P. Kallberg, S. Uppala, A. Hernandez, A. Nomura, and E. Serrano (1997), ECMWF re-analysis project report series: 1. ERA description, 84 pp., Eur. Cent. for Med. Range Weather Forecasts, Reading, UK.

Gruber, N., M. Gloor, S. Fan, and J. L. Sarmiento (2001), Air-sea flux of oxygen estimated from bulk data: Implications for the marine and atmospheric oxygen cycles, *Global Biogeochem. Cycles*, *15*, 783–803.

Hamme, R. C., and S. R. Emerson (2002), Mechanisms controlling the global oceanic distribution of the inert gases argon, nitrogen and neon, *Geophys. Res. Lett.*, *29*(23), 2120, doi:10.1029/2002GL015273.

Haney, R. L. (1971), Surface thermal boundary conditions for ocean circulation models, *J. Phys. Oceanogr.*, *1*, 241–248.

Jenkins, W. J., and S. C. Doney (2003), The subtropical nutrient spiral, *Global Biogeochem. Cycles*, *17*(4), 1110, doi:10.1029/2003GB002085.

Jerlov, N. G. (1976), *Marine Optics*, Elsevier, New York.

Keeling, R. F., and S. R. Shertz (1992), Seasonal and interannual variations in atmospheric oxygen and implications for the global carbon cycle, *Nature*, *358*, 723–727.

Keeling, R. F., B. B. Stephens, R. G. Najjar, S. C. Doney, D. E. Archer, and M. Heimann (1998), Seasonal variations in the atmospheric $O_2/N_2$ ratio in relation to the kinetics of air-sea gas exchange, *Global Biogeochem. Cycles*, *12*, 141–163.

Levitus, S. (1982), Climatological atlas of the world ocean, *NOAA Prof. Pap. 13*, 173 pp., U.S. Gov. Print. Off., Washington, D. C.

Levitus, S., and T. P. Boyer (1994), *World Ocean Atlas 1994*, vol. 4, *Temperature*, *NOAA Atlas NESDIS 4*, U.S. Gov. Print. Off., Washington, D. C.

Levitus, S., R. Burgett, and T. P. Boyer (1994), *World Ocean Atlas 1994*, vol. 3, *Salinity*, *NOAA Atlas NESDIS 3*, U.S. Gov. Print. Off., Washington, D. C.

Madec, G., P. Delecluse, M. Imbard, and C. Lévy (1998), OPA 8.1 ocean general circulation model reference manual, 91 pp., *Note Pôle Model. 11*, Inst. Pierre-Simon Laplace, Paris.

Marshall, J., A. Adcroft, C. Hill, L. Perelman, and C. Heisey (1997), A finite-volume, incompressible Navier Stokes model for studies of the ocean on parallel computers, *J. Geophys. Res.*, *102*, 5753–5766.

Najjar, R. G., and R. F. Keeling (2000), Mean annual cycle of the air-sea oxygen flux: A global view, *Global Biogeochem. Cycles*, *14*, 573–584.

Oschlies, A. (1999), An unrealistic high-salinity tongue simulated in the tropical Atlantic: Another example illustrating the need for a more careful treatment of vertical discretizations in OGCMS, *Ocean Model.*, *1*, 101–109.

Oschlies, A. (2000), Equatorial nutrient trapping in biogeochemical ocean models: The role of advection numerics, *Global Biogeochem. Cycles*, *14*, 655–667.

Oschlies, A., and V. Garçon (1999), An eddy-permitting coupled physical-biological model of the North Atlantic: 1. Sensitivity to advection numerics and mixed layer physics, *Global Biogeochem. Cycles*, *13*, 135–160.

Oschlies, A., and P. Kähler (2004), Biotic contribution to air-sea fluxes of $CO_2$ and $O_2$ and its relation to new production, export production, and net community production, *Global Biogeochem. Cycles*, *18*, GB1015, doi:10.1029/2003GB002094.

Oschlies, A., W. Koeve, and V. Garçon (2000), An eddy-permitting coupled physical-biological model of the North Atlantic: 2. Ecosystem dynamics and comparison with satellite and JGOFS local studies data, *Global Biogeochem. Cycles*, *14*, 499–523.

Pacanowski, R. C., and S. M. Griffies (1999), *The MOM 3 Manual*, Geophys. Fluid Dyn. Lab., Princeton, N. J.

Paulson, C. A., and J. J. Simpson (1977), Irradiance measurements in the upper ocean, *J. Phys. Oceanogr.*, *7*, 952–956.

Sheng, J., D. G. Wright, R. J. Greatbatch, and D. E. Dietrich (1998), CANDIE: A new version of the Diecast Ocean Circulation Model, *J. Atmos. Oceanic Technol.*, *15*, 1414–1432.

Simonot, J. Y., and H. Le Treut (1986), A climatological field of mean optical properties of the world ocean, *J. Geophys. Res.*, *91*, 6642–6646.

Smith, R. D., J. K. Dukowicz, and R. C. Malone (1992), Parallel ocean general circulation modelling, *Physica D*, *60*, 38–61.

Spitzer, W. S., and W. J. Jenkins (1989), Rates of vertical mixing, gas exchange and new production: Estimates from seasonal gas cycles in the upper ocean near Bermuda, *J. Mar. Res.*, *47*, 169–196.

Stephens, B. B., R. F. Keeling, M. Heimann, K. D. Six, R. Murnane, and K. Caldeira (1998), Testing global ocean carbon cycle models using measurements of atmospheric $O_2$ and $CO_2$ concentration, *Global Biogeochem. Cycles*, *12*, 213–230.

Wanninkhof, R. (1992), Relationship between wind speed and gas exchange over the ocean, *J. Geophys. Res.*, *97*, 7373–7382.

Webb, D. J., B. A. de Cuevas, and C. S. Richmond (1998), Improved advection schemes for ocean models, *J. Atmos. Oceanic Technol.*, *15*, 1171–1187.

Well, R., and W. Roether (2003), Neon distribution in South Atlantic and South Pacific waters, *Deep Sea Res., Part I*, *50*, 721–735.

H. Dietze, Leibniz-Institut für Meereswissenschaften an der Universität Kiel, Düsternbrooker Weg 20, D-24105 Kiel, Germany. (hdietze@ifm-geomar.uni-kiel.de)

A. Oschlies, School of Ocean and Earth Science, Southampton Oceanography Centre, Southampton SO14 3ZH, UK. (azo@soc.soton.ac.uk)